Thermal Behaviour Analysis of a Leading Edge Ribbed Channel Using Liquid Crystal Technique

Carlo Carcasci
Giacomo Migliorini
Dipartimento di Energetica "S. Stecco"
Università degli Studi di Firenze, Italy
Via S. Marta, 3 50139 - Firenze
Tel +39.055.4796575
Fax +39.055.4796342
e-mail: bobo@brun.de.unifi.it
carca@brun.de.unifi.it

Daniele Coutandin
Fiat Avio S.p.A.
Via Nizza, 312
10127 Torino, Italy
Tel. +39.011.6859560
e-mail: coutandin.daniele@fiatavio.it

ABSTRACT

The continuous developing of gas turbines as Aeroengines leads the designers to the reaching of higher performances in terms of increasing operating temperatures and lower emissions standards. Thus the necessity for more effective blade cooling, in order to maintain the metal temperature fields at levels consistent with blade design life, is required.

This work intends to give informations about the thermal behaviour of the fluid inside a turbine blade cooling system. We analysed a 5:1 model of an actual blade cooling system (leading edge ribbed channel) designed by FiatAvio, in order to retrieve the surface heat transfer coefficient distribution inside the model we used a transient method based on Thermochromic Liquid Crystal technique. To control the results provided from image analysis and data reduction we compared our results with those coming from correlations available in literature.

From image visualisation and surface heat transfer maps we are able to see how the geometry of the system influences the heat transfer inside the blade.

NOMENCLATURE

A	section	[m^2]
cp	specific heat	[J/(kgK)]
d_h	hydraulic diameter	$d_h = \frac{4A}{P}$ [m]
h	heat transfer coefficient	[W/(m^{2}K)]
k	thermal conductivity	[W/(mK)]
p	pressure	[Pa]
s	position across the thickness	[m]
P	perimeter	[m]
Re	Reynolds number	$\mathrm{Re} = \frac{u \cdot \rho \cdot d_h}{\mu}$
T	Temperature	[K]
t	time	[s]
u	velocity	[m/s]
x	position on the surface	[pixel]
y	position on the surface	[pixel]
α	thermal diffusivity	[m^2/s]
δ	wall thickness	[m]
μ	viscosity	[kg/(ms)]
ρ	density	[kg/m^3]

Paper presented at the RTO AVT Symposium on "Advanced Flow Management: Part B – Heat Transfer and Cooling in Propulsion and Power Systems", held in Loen, Norway, 7-11 May 2001, and published in RTO-MP-069(I).

Report Documentation Page			*Form Approved* *OMB No. 0704-0188*
Public reporting burden for the collection of information is estimated to average 1 hour per response, including the time for reviewing instructions, searching existing data sources, gathering and maintaining the data needed, and completing and reviewing the collection of information. Send comments regarding this burden estimate or any other aspect of this collection of information, including suggestions for reducing this burden, to Washington Headquarters Services, Directorate for Information Operations and Reports, 1215 Jefferson Davis Highway, Suite 1204, Arlington VA 22202-4302. Respondents should be aware that notwithstanding any other provision of law, no person shall be subject to a penalty for failing to comply with a collection of information if it does not display a currently valid OMB control number.			
1. REPORT DATE **00 MAR 2003**	2. REPORT TYPE **N/A**		3. DATES COVERED **-**
4. TITLE AND SUBTITLE **Thermal Behaviour Analysis of a Leading Edge Ribbed Channel Using Crystal Tehcnique**			5a. CONTRACT NUMBER
			5b. GRANT NUMBER
			5c. PROGRAM ELEMENT NUMBER
6. AUTHOR(S)			5d. PROJECT NUMBER
			5e. TASK NUMBER
			5f. WORK UNIT NUMBER
7. PERFORMING ORGANIZATION NAME(S) AND ADDRESS(ES) **NATO Research and Technology Organisation BP 25, 7 Rue Ancelle, F-92201 Neuilly-Sue-Seine Cedex, France**			8. PERFORMING ORGANIZATION REPORT NUMBER
9. SPONSORING/MONITORING AGENCY NAME(S) AND ADDRESS(ES)			10. SPONSOR/MONITOR'S ACRONYM(S)
			11. SPONSOR/MONITOR'S REPORT NUMBER(S)
12. DISTRIBUTION/AVAILABILITY STATEMENT **Approved for public release, distribution unlimited**			
13. SUPPLEMENTARY NOTES **Also see: ADM001490, Presented at RTO Applied Vehicle Technology Panel (AVT) Symposium held inLeon, Norway on 7-11 May 2001, The original document contains color images.**			
14. ABSTRACT			
15. SUBJECT TERMS			

16. SECURITY CLASSIFICATION OF:			17. LIMITATION OF ABSTRACT	18. NUMBER OF PAGES	19a. NAME OF RESPONSIBLE PERSON
a. REPORT **unclassified**	b. ABSTRACT **unclassified**	c. THIS PAGE **unclassified**	**UU**	**14**	

Standard Form 298 (Rev. 8-98)
Prescribed by ANSI Std Z39-18

Subscripts and superscripts

0 initial condition, position at $s=0$
av average
e exchanged

INTRODUCTION

The continuous increase in turbine inlet gas temperature in the aeronautical engines, leads to the need of more effective blade cooling in order to maintain the metal temperature field at temperature levels consistent with blade design life. This one could be obtained introducing new cooling technologies or modifying the existing one, increasing the efficiency of some critical areas. Both the solutions require being able to predict the local heat transfer effects within the cooling geometry and not only the mean values into the channels, as the normal correlations available in the literature give. Even if the introduction of CFD calculations in the design process of a turbine blade cooling system simplifies the knowledge of an internal flow field, for the thermal behaviour of the system we still need to have some experimental approach.

One of the most used methods is the liquid crystal technique, which has been introduced in FiatAvio some years ago. The need to have more detailed informations about the local heat transfer convective coefficients within blade cooling systems, and to reduce the time for data reduction, has required a new method for experimental data analysis.

The whole method allows the digital images conversion, the heat transfer equation integration and the heat transfer coefficients map showing. The code is realized with MATLAB®, this programming language suits well our needs, we can focus our attention on heat transfer problems only, because of the great, built – in, image editing functions availability. Moreover the high flexibility of the elaboration method makes it very suitable for industrial processes, which needs quick responses for the different solutions proposed during the designing phases. In the paper, we propose the results of this technique applied to a ribbed channel, they are compared with those coming from correlation available in literature (Han, 1985).

TESTED GEOMETRY

For this type of analysis a rotor blade of an LPT turbine of an Aeronautical Engine has been chosen. Main characteristics of this blade are summarized in Table 1 and shown in Figure 1. It consists of three-separated internal radial channel for convective cooling, which have, for the 2/3 of their height, turbulence promoters as inclined ribs on the two walls on the pressure and suction side. All the channels have a tip discharge and, in addition, the third one has a row of holes necessary for the trailing edge film cooling.

Parameter	**Units**	
Mean Height	mm	110
Mean Chord	mm	22
T.E. Holes number	-	56
T.E. Holes diameter	mm	0.38
Ribs Height	mm	0.2
Ribs Pitch	mm	2.0
Ribs Angle	mm	30

Table 1: Tested Geometry.

During the tests all the internal cooling system has been analysed; hereafter nevertheless, we focus our attention on the Leading Edge channel only. The channel has a quasi-triangular section, as highlighted in Figure 1, with the ribs that cover the corresponding internal Pressure and Suction Side

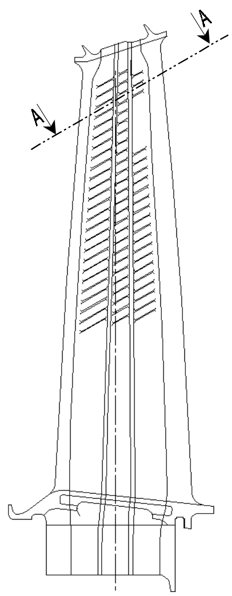

a

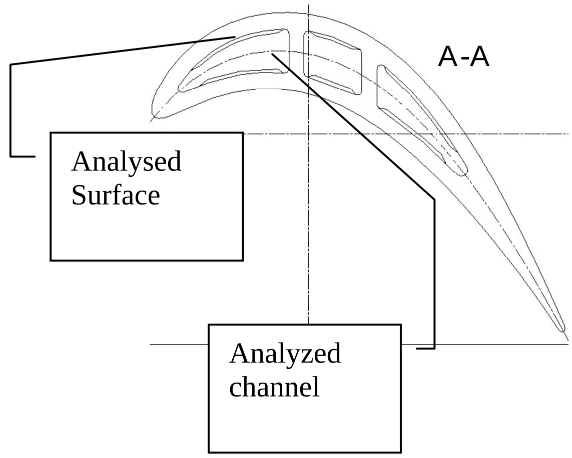

b

Figure 1: Blade internal cooling system: a) channels disposition; b) cross section, analysed surface.

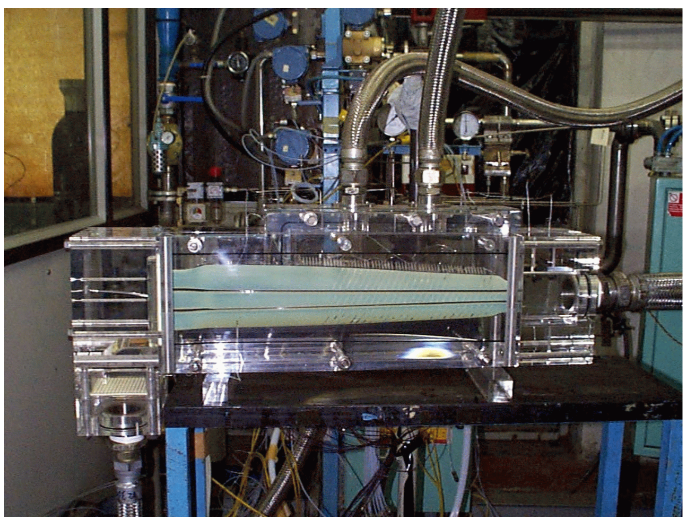

Figure 2: Experimental Rig.

EXPERIMENTAL FACILITY

Experiments were carried out in the FiatAvio laboratories in Turin (Italy), using a scaled 5:1 cooling system model. This model represents the whole internal cooling geometry of the blade, with ribs and Trailing Edge holes. It has been manufactured using PMMA material that has a good optical access and a low thermal conductivity. In the Figure 2 the whole model is shown; on the left side there is the blade root and on the right side, the tip. The leading edge is on the bottom side.

There are three independent air intake sections (one for each channel) and two independent exits (trailing edge film cooling holes and tip) with mass flow rate measurement. In this way we can test each channel separately, in every flow rate condition.

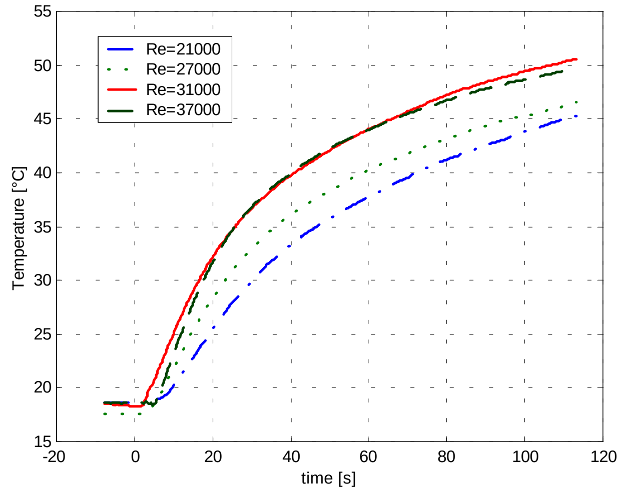

Figure 3: Air Temperature variation inside the model.

Internal channels are instrumented with 21 thermocouples for the air temperature measurements within the model. There are also two "wall thermocouples" to verify the liquid crystal temperature wall measurements. Figure 3 reports air temperature during the four tests, measured from the thermocouple positioned in the area of interest.

Pressure can be measured with ten pressure taps during all tests, at the inlet and exit of each channel.

Similitude model and actual blade has to be verified, Reynolds and Mach numbers constancy is observed. So, since our model is 5:1 scaled and temperature is fixed by liquid crystal characteristics, we have to operate with the pressure values reported in Table 2.

Four tests have been carried out using four different Reynolds numbers. Those values have been obtained using values of inlet and outlet pressure less than the atmospheric one. Table 2 summarizes the main test parameters:

	Inlet Total Pressure	**Reynolds Number**
TEST 1	46.19 kPa	21000
TEST 2	51.30 kPa	27000
TEST 3	53.90 kPa	31000
TEST 4	59.87 kPa	37000

Table 2: Test conditions.

THE LIQUID CRYSTAL TECHNIQUE

The advantages of using Liquid Crystals as surface temperature sensors are well known (Camci – 1992, Taslim – 1988, Graham- 2000); they are particularly able to completely describe the whole test surface providing careful temperature measurements. The whole temperature field is controlled recording the iso-temperature lines movements. We used thermal sensitive paints; they are monochromatic and vary their grey intensity at a certain surfaces temperature.

The data analysis and reduction technique consists of three main parts:

1. Data acquisition;
   a. Digital camera recording of test;
   b. Pressure and temperature data acquisition;
2. Image acquisition, digital frame grabbing on PC;
3. Image digital elaboration
   a. Transformation of Images in to a numerical matrix;
   b. Matrix numerical elaboration, heat transfer coefficient evaluation;

The main target is to come to convection heat transfer coefficient evaluation through a movie, and so an images set, of the surface heating. The image set describes the whole temperature changes along time. For each point on the surface we have the complete grey intensity vs. time curve.

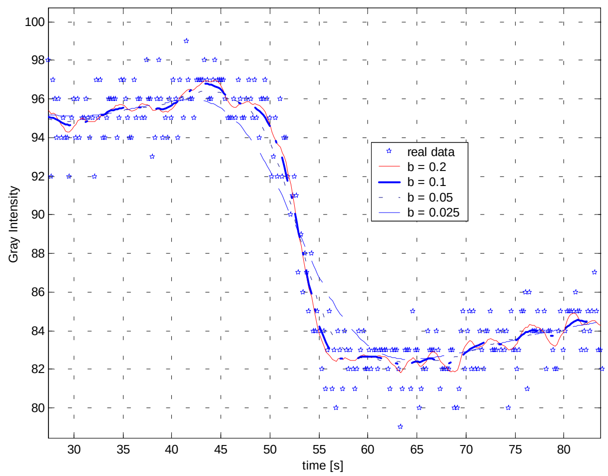

Figure 4: Grey Intensity vs. time Curve on a pixel.

In order to determine heat transfer coefficient, time when the surface reaches a certain temperature has to be found. The first step is to come to the curve of grey intensity in time. Figure 4 shows this curve, plotted as real and filtered data. A MATLAB® function (Digital Signal Processing Toolbox® – filtfilt.m function), in order to eliminate the data dispersion, is used. The curve is determined by the liquid crystal characteristics, it presents a flex point.

Using the real data curve in order to find this point it is almost impossible, since it presents a great number of flex points due to its continuous changes in concavity; it is necessary to filter the data. The function used is a digital filtering function with no shift in phase between input and output. Factor *b* is the numerator's vector of coefficients of the transfer function, which links input to output. It can be seen that the smaller is *b* the smoother is the resulting filtered curve.

From the liquid crystal characteristics it is known that the curve passes through this point when the temperature of the surface, where they are applied on, reaches the value of 32.5°C.

From the movie analysis for each point on the image we obtain a curve like that one shown in Figure 4 and from each curve it can be found a flex instant. Thus we obtained the temperature (32.5 °C) at a certain instant, instant that changes depending on the position on the surface.

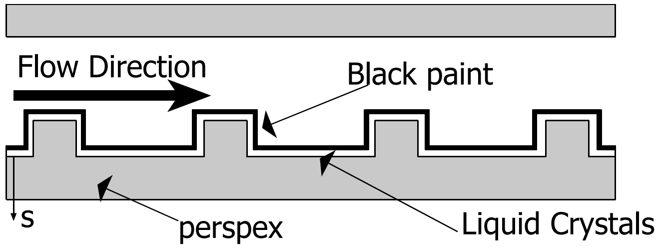

Figure 5: Channel section.

Heat Transfer Computational Model

To determine the heat transfer coefficient, unsteady Fourier equation is solved (Holmann, 1990) imposing thermal conductibility constancy:

$$\nabla^2 T = \frac{1}{\alpha}\frac{\partial T}{\partial t} \text{ , } k(T)=cost \ \forall T \text{ , } \alpha = \frac{k}{\rho c_p} \qquad \text{Eq. 1}$$

We considered only convection and conduction heat transfer, in our problem the radiation one is negligible.

Considering also thermal conductibility very low and isotropic material, Eq. 1 becomes (conduction is one-dimensional in the *s* direction):

$$\frac{\partial^2 T(s,t)}{\partial s^2} = \frac{1}{\alpha}\frac{\partial T(s,t)}{\partial t} \qquad \text{Eq. 2}$$

Which is solved in respect with the following initial condition:

$$t=0 \ \Rightarrow \ T(s,0)=T(\delta,0)=T_0, \ \forall \text{s} \qquad \text{Eq. 3}$$

Each point of the model has the same temperature at time $t=0$.

And with the following boundary conditions (convection heat transfer on the internal wall, adiabatic condition on the internal wall):

$$s=0 \ \Rightarrow \ \dot{q}_e = -k\left(\frac{\partial T(s,t)}{\partial s}\right)_{s=0} = h\left[T_g(t)-T(0,t)\right], \ \forall t \qquad \text{Eq. 4}$$

$$s=\delta \ \Rightarrow \ \dot{q}_e = -k\left(\frac{\partial T(s,t)}{\partial s}\right)_{s=\delta} = 0 \quad \Rightarrow \left(\frac{\partial T(\delta,t)}{\partial s}\right) = 0 \text{ , } \forall t \qquad \text{Eq. 5}$$

If gas temperature would be constant we could solve analytically the problem integrating in a closed form Eq. 2 but, since T_g varies with time, we have to integrate it, in *x* and *t*, with common second order finite differences methods (Holmann, 1990) once we know the initial ambient temperature, which is the temperature of air and model at test starting, and the air temperature ($T_{air}=T_g(t)$, see Figure 3) during the whole test. The heat transfer coefficient determination process is iterative since it is our problem unknown value.

Space below ribs is not treated because of the lacking of 1D assumption.

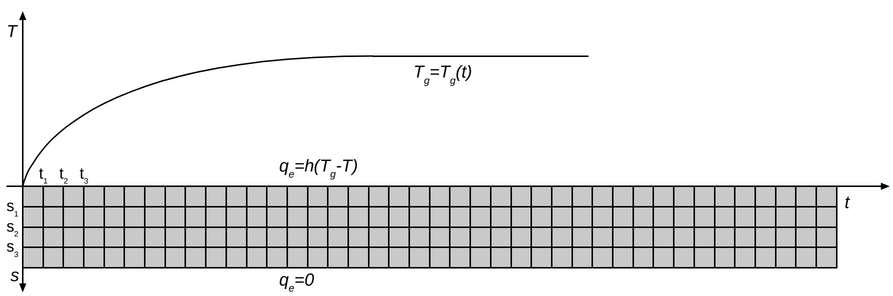

Figure 6: Integration domain for a point, varying time.

Figure 6 shows the integration domain for a point on the surface, the *s* axis identifies the position across the external wall and the *t* axis is the time axis.

Procedure for data analysis

The whole procedure is developed for an easy and quick data analysis.

At first the movie of the test has to be split in its elementary frames, this is easy to do with a simple image acquisition program or directly on the image acquisition board. Each movie frame is saved as a different image; typically there will be 25 images for each second of test (PAL format). The whole set of frames is now ready to be analysed.

The code inputs are:

1. Temperature inputs:
    a. Ambient temperature, at time $t=0$;
    b. Air flow temperature, function of time and position inside channel acquired by system.
    c. Liquid Crystal Characteristic Temperature (32.5 °C).

2. Material inputs:
   a. Density.
   b. Specific heat.
   c. Thermal conductivity.
3. Time inputs:
   a. Frame number corresponding to time $t=0$;
   b. Time vector corresponding to acquired airflow temperatures.

The code is structured in the following main steps:

1. Transformation of each image in a 2D matrix where each element has the grey value of the image pixel with the same coordinates. The number of acquired images depends on:
   a. Test duration.
   b. Frame rate of adopted video system (European video system is PAL: frame rate equal to 25 frame per second)
   c. Time step given to the code (for example one could decide to acquire not all the frame but only one every five frames in order to increase the calculation speed).
2. Image gridding: determination of points where we are going to evaluate the heat transfer coefficient, at most the point number can be equal to the image number of pixels.
3. Image Numerical analysis:
   a. Evaluation of grey function of time curve for each grid point
   b. Flex point determination. Time interval determination, from test starting to flex instant, this is the time in which the surface reaches the temperature of 32.5°C (Turning Time).
4. Heat transfer analysis:
   a. Imposition of a guess value for heat transfer coefficient;
   b. Fourier equation integration in time, determination of surface temperature at the turning time.
   c. Surface temperature check, if it corresponds to the liquid crystal calibration temperature (32.5°C) we found *h*, otherwise we have to start again from point 4.b, after the imposition of a new h value.
5. The whole process, from point 3, for each point defined in point 2, is repeated.
6. Results saving:
   a. Heat transfer coefficients map,
   b. Turning time distribution.
7. Results interpolation and plotting.

Several code personalizations are possible (time step, number of point across the wall thickness, number of point analysed on the surface) in order to increase calculation speed or accuracy.

EXPERIMENTAL RESULTS

Each test has been filmed using a digital camera. In order to increase the images definition and to put in evidence the local phenomena between the ribs, only the area near the region of interest has been investigated.
In Figure 7 is shown an example of the liquid crystal paint melting sequence.
The dark spots show the melted paint and indicate, then, higher convective heat transfer coefficients.

t=5 s

t=10 s

t=15 s

t=20 s

t=25 s

Figure 7: Frames showing test evolution Re=31000.

DATA REDUCTION

The code flexibility allows performing several data analysis. The code evaluates the heat transfer coefficient in discrete points (pixels), and then interpolates, in order to shorten the calculation time, the found values, obtaining the final map of the analysed area. In this analysis is pointed out how the code can be used for focusing the attention of the designers on the whole channel or only on part of it. At last we give a comparison between our data reduction code (CriLiq) and correlations available in literature (Han, 1985).

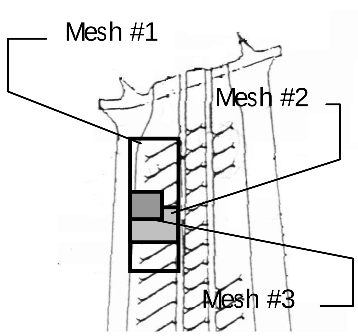

Figure 8: Analysed area inside channel, Mesh #1, #2, #3.

Mesh	Dimensions [mm]
Mesh #1	40 x 110
Mesh #2	39 x 27
Mesh #3	16 x 17

Table 3: Meshes used for analysis.

Figure 8 shows the three meshes used for analysing the channel and for the comparison with correlations codes. The mesh #1 has been chosen in order to verify the mean behaviour of the heat exchange and compare it with the normal correlations available in literature and normally referred to standard geometries (i.e. square section channels). The resulting heat transfer coefficient values matrix has 16 columns, one for each position across the channel, from beside the mid channel to the leading edge wall.

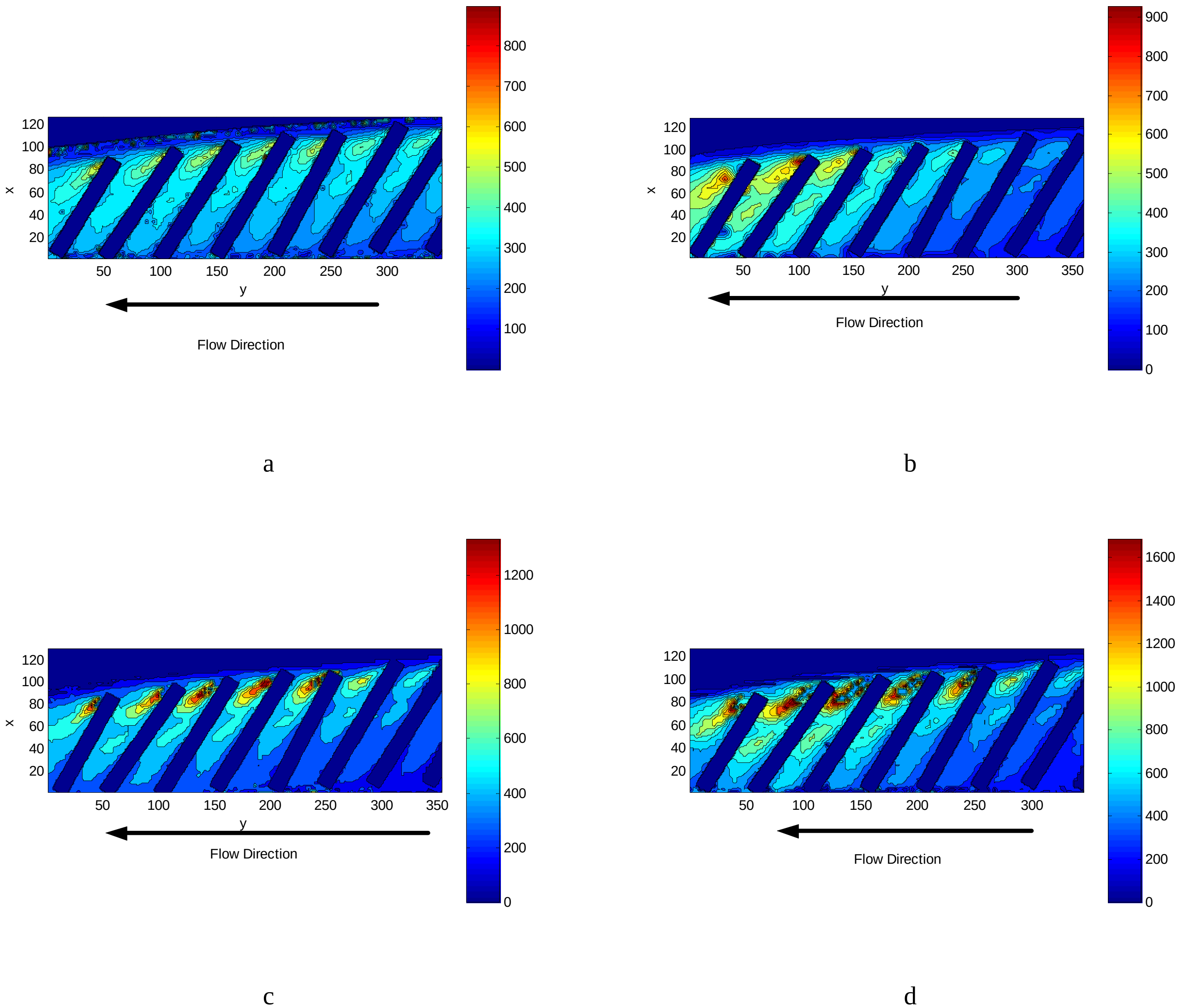

Figure 9: Heat transfer coefficient map [W/(Km^2)], a) Re=21000, b) Re=27000, c) Re=31000, d) Re=37000 mesh #1.

Results of the four tests performed at the different Reynolds number have been reported in Figure 9 (a, b, c and d) as convective heat transfer coefficients distribution. The fringe plot post-processing allows us to immediately highlight the high heat exchange values in the region immediately behind the ribs near the leading edge side.

This appeared clear even from a first look to the test images Figure 7. Here is visible the “melting direction” is more or less parallel to the ribs even to cover the whole space.

The ribs leave a smooth narrow passage beside the leading edge wall of the channel. A detail in the last picture of Figure 7 shows that in a region between the blade leading edge and the ribs, the paint reaches the melting temperature in longer time than other channel areas. This indicates a very low heat transfer coefficient and can be correlated, as described, at the smooth geometry of this “corner”.

The ribs form, with the wall, a nozzle shape passage for the flow. The flow, going beyond a rib, passing through the space between the leading edge side of the rib and the leading edge wall of the channel is accelerated and, here, is probably characterized by high turbulence levels with recirculation and flow separation. The natural turbulence created by ribs is increased. The effect is probably emphasized by channel triangular cross section. It is therefore immediately clear as in the thin region, between the ribs and the side of the channel near the blade leading edge, corresponding to a smooth narrow area of the channel, low values of heat Transfer coefficients have been evaluated.

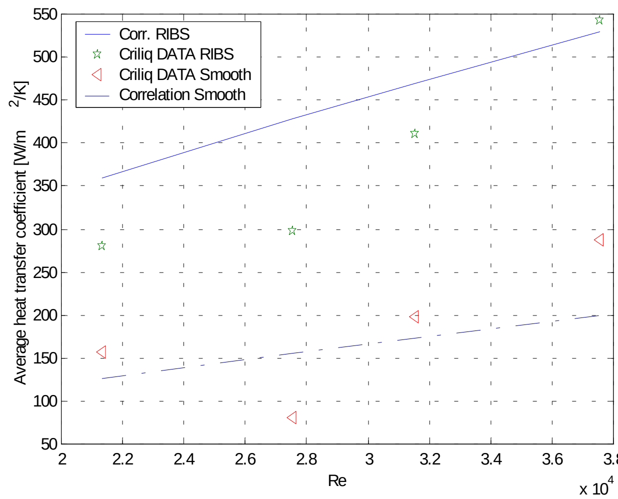

Figure 10:Comparison with standard correlations.

In order to evidence the decrease in heat exchange, mean heat transfer coefficient values have been calculated for the two regions, the ribbed and the smooth one, and reported, vs. the Reynolds number, in the graph in Figure 10. Experimental data are there compared with values calculated using standard correlations both for ribbed (Han, 1985) and smooth (Colburn, Ozisik - 1995) channels. In both cases we can observe a good agreement between experimental and calculated values. It is clear the importance of an investigation in the smooth area because, even if this area is very small if compared to the whole channel, it is therefore true that this is the area in which a designer would like to have the maximum possible number of informations, in order to verify if heat exchange is satisfactory in a such delicate zone for blade cooling.

We have also to remember that Han correlations have been developed for square ducts where hydraulic diameter coincides with distance between two opposite ribs, and we treated the smooth region as a real smooth duct while there is mass exchange with the ribbed one.

We have reported correlations heat transfer coefficients only to control those obtained with our method. Average values are plotted with Reynolds number (evaluated for the duct hydraulic diameter - d_h).

Figure 8 shows also the calculation grids used for the other analyses done.

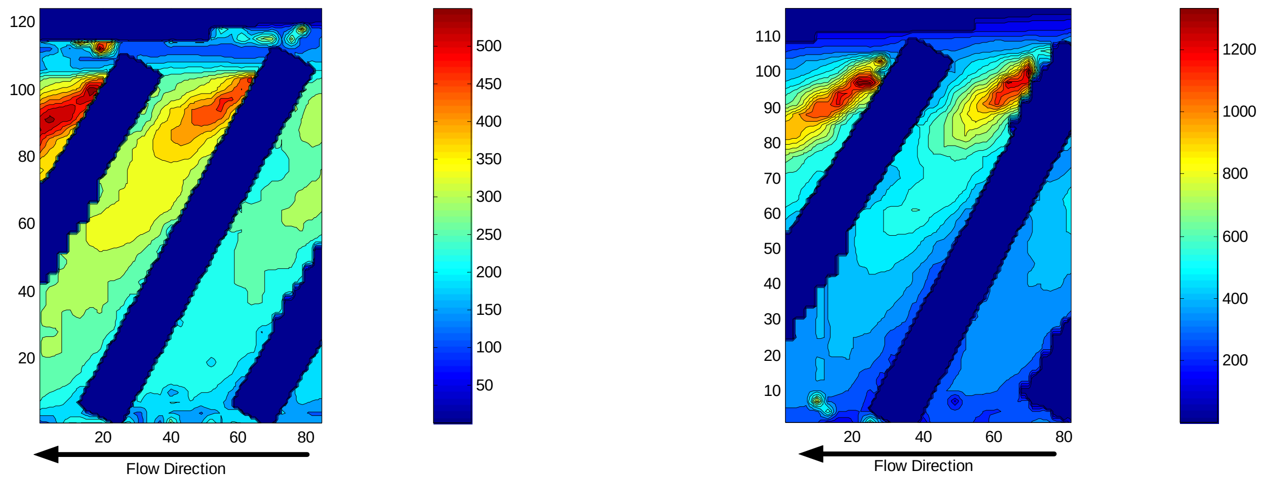

a b

Figure 11: Detailed sketch of channel htc [W/(Km^2)] distribution, a) Re=21000, b) Re=31000 mesh #2.

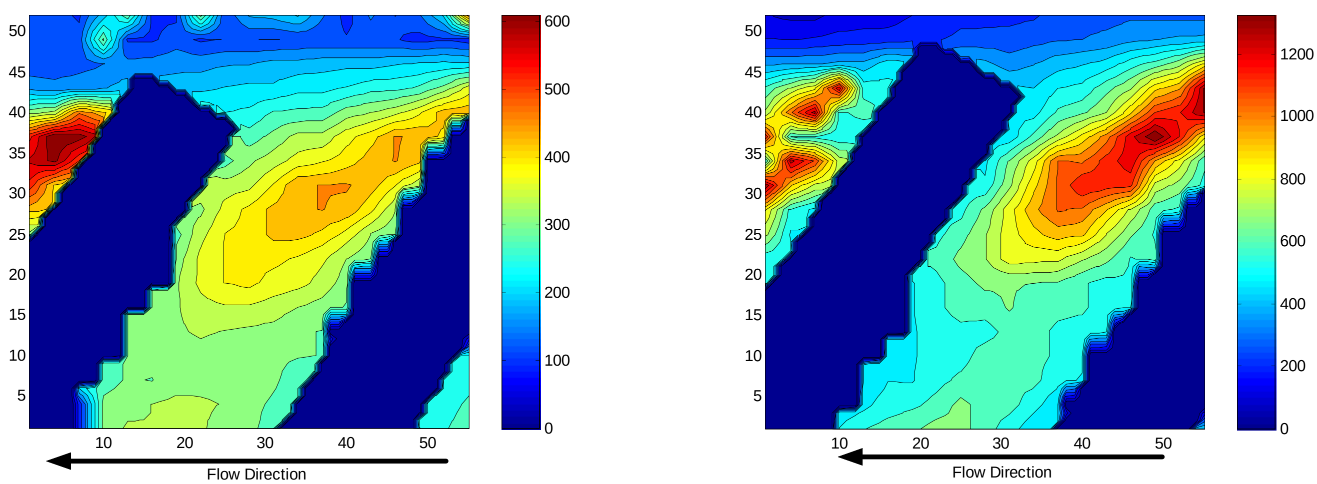

a b

Figure 12: Detail of htc [W/(Km^2)] distribution between two ribs a) Re=21000, b) Re=31000, mesh #3.

From Figure 11 (a, b) to Figure 12 (a, b) are shown particularly detailed analyses that investigate the particular nature of the flow between two contiguous ribs at two different Reynolds number, mainly we have pointed out the presence of high turbulence level and high heat transfer coefficient values at the ribs end. The position of the higher heat transfer coefficient value is in good agreement with other experimental results found in literature (Caçan, 1998). The high heat transfer coefficient zone seems to be modified and closer to the rib's end if compared with results referring to square or rectangular ducts.

The maps show in detail the increase in HTC moving to the leading edge wall and the sudden decrease in the smooth zone between the end of the ribs and the L.E. wall.

CONCLUSIONS

With the present study we have developed a tool (CriLiq) that allows us to evaluate the heat transfer coefficient from data coming from liquid crystal tests.

The tool is very flexible and allows a complete tested surface analysis, evaluating heat transfer coefficient as both an average value along a direction or inside an area and as a punctual value. It helps the designer also in visualizing flow behaviour inside the channel with a qualitative description.

During the trial phase it showed a good agreement with standard correlation whether in the smooth zone or in the ribbed one.

Moreover it shows an high sensitivity to the air temperature values, so it is very important and delicate its measuring for the heat transfer coefficient reliability.

If the investigated domain is large and the gridding dense the calculation time become long.

REFERENCES

Anil, K.J., “Fundamentals of image processing”, Prentice – Hall International Editions.

AA., VV., 1998,“Matlab User’s Guide – Version 4.2”, The MathWorks Inc.

Camci, C., Kim, K., Hippensteele, S.A., “A new hue capturing technique for the quantitative interpretation of liquid crystal images used in convective heat transfer studies”, (1992), Journal of Turbomachinery, 114, 765-775.

Carcasci C., Facchini B., Ferrara G., 1995 " A Rotor Blade Cooling Design Method For Heavy Duty Gas Turbine Applications". ASME paper 95-CTP-90 VIII° ASME Cogenturbo, Agosto 1995, Vienna, Austria.

Carcasci C., Facchini B., Corradini U., 1996. “Il Raffreddamento Delle Turbine A Gas Heavy Duty: Criteri Di Progetto Di Palettature E Componenti Secondari”. Atti del “Turbomacchine ‘96”. Genova, Luglio 1996.

Florschuetz, L.W., Isoda, Y., 1983 ; "Flow Distributions and Discharge Coefficient Effects for Jet Array Impingement With Initial Crossflow", ASME J. of Engineering for Power, 1983, vol.105, pp.296-304

Graham, D., Jeff, R., (2000) “The determination of transient wall heating experiments for the determination of convective heat transfer using liquid crystal Thermography”, Proceedings of Asme Turbo Expo 2000.

Han, J. C., Lei, C. K., 1983, “Heat Transfer and Friction in Square Ducts with Two Opposite Rib-Roughened Walls,” ASME Paper 83-HT-26.

Han, J. C., Park, J. S., Lei, C. K., 1985, “Heat Transfer Enhancement in Channels With Tubulence Promoters”, ASME Journal of Engineering for Gas Turbines and Power, Vol. 107, pp. 628-635.

Holmann, J. P., (1990) “Heat Transfer”, Mc Graw Hill.

Metzger, D. E., Haley, S. W., 1982, “ Heat Transfer Experiments and Flow Visualization for Arrays of Short Pin Fins”, ASME Paper 82-GT-138

Morris, W., Ayhan, T., 1984, “ An Experimental Study of Turbolent Heat Transfer in a Tube wich Rotates about an Orthogonal Axis”, Raccolta: Heat and Mass Transfer in Rotating Machinery, edited by Metzger, D.E., Afgan, N. H.

OzisiK, M.,N., 1995,“Heat Transfer: A Basic Approach”, McGrawHill.

Rau, G., Caçan, M., Moeller, D., Arts, T., “The effect of periodic ribs on the local aerodynamic and heat transfer performance of a Straight cooling channel” J. of Turbomachinery, Vol. 120, April, 1998, pp. 368-375.

Taslim, M. E. and Spring, S. D., 1988a, “An Experimental Investigation Of Heat Transfer Coefficients And Friction Factors In Passages Of Different Aspect Ratio Roughened With 45° Turbulators” proceedings of ASME National Heat Conference, Houston, TX.

Paper Number : 1

Name of Discusser: P. Ireland, University of Oxford

Question:
The rib heat transfer can contribute significantly to the total heat transfer for the passage.
Do you have any plan to measure rib heat transfer?

Answer:
Main goal of our work was to develop an integrate procedure for data analysis, so the rib heat exchange could be negligible.
For a complete understanding of the thermal behaviour, other solutions (e.g. metallic ribs) could be introduced in future.

Name of Discusser: B. Simon, MTU Aero Engines Munich

Question:
What was the error in gas temperature and how affected the gas temperature error the accuracy of the htc.?

Answer:
Error in gas temperature was below 0,5 ˚C and the influence in heat transfer coefficient value was below 10 %.

Name of Discusser: K. Patel, Pratt & Whitney Canada, Mississauga, Ont.

Question:
This is a powerful technique to determine heat transfer information on a static rig. How to use the data for rotational effects in a real turbine environment.

Answer:
The rig simulates only static conditions. Results will be compared with CFD codes and using this type of analysis rotational effects will be taken into account.

This page has been deliberately left blank

Page intentionnellement blanche